Hydrothermal Synthesis and Structural Characterization of $(NH_4)GaPO_4F$, KTP-type and $(NH_4)_2Ga_2(PO_4)(HPO_4)F_3$, Pseudo-KTP-type Materials

T. Loiseau,[†] C. Paulet,[†] N. Simon,[†] V. Munch,[‡] F. Taulelle,[‡] and G. Férey*[,†]

Institut Lavoisier, UMR CNRS 8637, Université de Versailles-St-Quentin en Yvelines, 45, Avenue des Etats-Unis, 78035 Versailles Cedex, France, and Laboratoire de RMN et Chimie du Solide, UMR 7510 ULP-Bruker-CNRS, Université Louis Pasteur, 4 rue Blaise Pascal, Strasbourg Cedex, France

Received November 17, 1999. Revised Manuscript Received January 13, 2000

Two new fluorinated gallium phosphates have been hydrothermally synthesized in the system $GaOOH/H_2O/H_3PO_4/HF$/guanidine or NH_4F (180 °C, autogenous pressure, 4 days). The structures of both compounds have been characterized by single-crystal X-ray diffraction. The $(NH_4)GaPO_4F$ phase is isostructural with the $KTiOPO_4$ (KTP) structural type. The structure of the second phase $(NH_4)_2Ga_2(PO_4)(HPO_4)F_3$, named pseudo-KTP or p-KTP, is closely related to that of KTP. In the latter, the existence of terminal P−OH and Ga−F bond along the *b* axis prevents the full connection by corner-sharing of the PO_4 and $Ga(O,F)_6$ units as it occurs in KTP structure. It results in a more distorted framework in which the occluded ammonium cations interact mainly with the P−OH and Ga−F terminal bonds. The structure of p-KTP was examined by ^{19}F and ^{31}P solid-state nuclear magnetic resonance spectroscopy using high-speed MAS experiments (30 kHz). ^{19}F NMR indicates a full occupancy by fluorine for the atomic sites bridging the gallium atoms. Crystal data for $(NH_4)GaPO_4F$: orthorhombic, space group $Pna2_1$ (no. 33), $a = 12.9207(2)$ Å, $b = 6.440(1)$ Å, $c = 10.4147(2)$ Å, $V = 866.60(3)$ Å^3, $Z = 8$, R1 = 0.0279%, wR2 = 0.0785 for 2216 reflections with $I > 2\sigma(I)$. Crystal data for $(NH_4)_2Ga_2(PO_4)(HPO_4)F_3$: orthorhombic, space group $Pna2_1$ (no. 33), $a = 12.4967(2)$ Å, $b = 7.7015(1)$ Å, $c = 9.8463(1)$ Å, $V = 947.67(2)$ Å^3, $Z = 4$, R1 = 0.0406, wR2 = 0.0985 for 2820 reflections with $I > 2\sigma(I)$.

Introduction

The research on phosphate materials with new open frameworks is currently in progress due to their potential applications in catalysis, in gas separation, or as ion exchangers.[1,2] In this course, the addition of fluoride anions into the reaction mixture, developed by Guth and Kessler,[3] has led to the discovery of new microporous structural types, some of them exhibiting very large channels as in cloverite,[4] ULM-5[5] or ULM-16.[6] In these phases, fluorine is either trapped within a double 4-ring cage (D4R) or participates to the coordination sphere of the metal atom; its coordination is increased to five (trigonal bipyramid)) or six (octahedron). A systematic study of the fluorine systems[7] has shown that the geometry of the structure-directing agent plays an important role for the elaboration of 3D open framework. It has been observed that the ammonium groups of the organic molecules interact preferentially with the fluorine atoms of the framework via hydrogen bonds.

To specify the relationships between the template and the fluorine atoms, we focused our attention on a nitrogen-rich molecule as the guanidinium cation, $C(NH_2)_3^+$. This molecule has already been used in the synthesis of new phosphates[8] or fluorides[9,10] in which it has a countercation role. It is also a good candidate as structure-directing agent for the preparation of aluminum,[11] vanadium,[12,13] and zinc phosphates.[14−16] The aluminum or vanadium phosphates exhibit 2D or 1D structures, whereas the zinc compounds are characterized either by new three-dimensional frameworks containing 12- or 18-membered rings or related zeolite structural type. In this context, we undertook the study

* Author for correspondence. E-mail: ferey@chimie.uvsq.fr.
† Université de Versailles-St-Quentin en Yvelines.
‡ Université Louis Pasteur.

(1) Cheetham, A. K.; Férey, G.; Loiseau, T. *Angew. Chemie, Int. Ed.* **1999**, *38*, 3268.
(2) Davis, M. E. *Chem. Eur. J.* **1997**, *3* (11), 1745.
(3) Guth, J. L.; Kessler, H.; Wey, R. *Stud. Surf. Sci. Catal.* **1986**, *28*, 121.
(4) Estermann, M.; McCusker, L. B.; Baerlocher, C.; Merrouche, A.; Kessler, H. *Nature* **1991**, *352*, 320.
(5) Loiseau, T.; Férey G. *J. Solid State Chem.* **1994**, *111*, 403.
(6) Loiseau, T.; Férey G. *J. Mater. Chem.* **1996**, *6* (6), 1073.
(7) Férey, G. *J. Fluorine Chem.* **1995**, *72*, 187. Férey, G. *C. R. Acad. Sci. Paris, Sér. IIc* **1998**, *1*, 1.
(8) Schülke, U.; Averbuch-Pouchot, M. T. *Z. Anorg. Allg. Chem.* **1995**, *621*, 1232.
(9) Bukovec, P. *Monatsh. Chem.* **1983**, *114*, 277.
(10) Fourquet, J. L.; Plet, F.; De Pape, R. *Rev. Chim. Mineral.* **1986**, *23*, 183.
(11) Bircsak, Z.; Harrison, W. T. A. *Chem. Mater.* **1998**, *10*, 3016.
(12) Bircsak, Z.; Harrison, W. T. A. *Inorg. Chem.* **1998**, *37*, 3204.
(13) Bircsak, Z.; Hall, A. K.; K. Harrison, W. T. A. *J. Solid State Chem.* **1999**, *142*, 168.
(14) Harrison, W. T. A.; Phillips, M. L. F. *Chem. Commun.* **1996**, 2771.
(15) Harrison, W. T. A.; Phillips, M. L. F. *Chem. Mater.* **1997**, *9*, 1837.
(16) Chippindale, A. M.; Cowley, A. R.; Peacock, K. J. *Microporous Mesoporous Mater.* **1998**, *24*, 133.

10.1021/cm991177z CCC: $19.00
Published on Web 05/15/2000

of the role of the guanidinium cation in the formation of microporous gallium phosphate in the presence of fluorine. The first results showed that this organic species easily decomposed into ammonium groups under hydrothermal conditions (150−180 °C, heating for 1−4 days). It leads to the formation of rather dense phases in which the ammonium groups are occluded.

We describe in this paper the preparation, the X-ray single-crystal analysis and the ^{19}F, ^{31}P MAS NMR characterizations of new fluorinated gallophosphates $(NH_4)_2Ga_2(PO_4)(HPO_4)F_3$ and $(NH_4)GaPO_4F$. The latter is isostructural with the well-known KTP type.[17] The structures of both compounds are closely related and we propose to hereafter label $(NH_4)_2Ga_2(PO_4)(HPO_4)F_3$ as pseudo-KTP or p-KTP.

Experimental Section

Synthesis. The syntheses of $(NH_4)_2Ga_2(PO_4)(HPO_4)F_3$ and $(NH_4)GaPO_4F$ materials were carried out hydrothermally in a 23-mL Teflon-lined stainless steel Parr bomb under autogenous pressure. These phases are obtained by using guanidinium carbonate which is decomposed into ammonium cations during the hydrothermal reaction. The p-KTP solid can be synthesized with ammonium fluoride instead of using guanidine. The starting reactants were gallium oxyhydroxide (GaO(OH), prepared by direct reaction of gallium metal with water at 220 °C under autogenous pressure for 3 days), phosphoric acid (H_3PO_4, Prolabo R.P. Normapur, 85%), fluorhydric acid (HF, Prolabo R.P. Normapur, 48%), carbonate guanidinium ($[2H_2NC(=NH)NH_2 \cdot H_2CO_3]$, Aldrich, 99%, noted GUA) or ammonium fluoride (NH_4F, Prolabo R.P. Normapur AR), and distilled water.

For $(NH_4)_2Ga_2(PO_4)(HPO_4)F_3$ or p-KTP, the molar ratio was 1 GaO(OH) (0.713 g)/1 H_3PO_4 (0.5 mL)/1 HF (0.25 mL)/0.5 GUA (0.315 g)/40 H_2O (4.25 mL). GaO(OH) was added to water, and then, H_3PO_4, HF, and GUA were successively added. The resulting pH of the solution was 3, and the mixture was placed in the autoclave at 180 °C for 4 days. $(NH_4)_2Ga_2(PO_4)(HPO_4)F_3$ was obtained as a pure phase. The crystalline product was filtered off, washed with distilled water, and dried at room temperature. With ammonium fluoride replacing the guanidine, the same solid is obtained by using the molar mixture: 1 GaO(OH) (0.713 g)/1 H_3PO_4 (0.5 mL)/1 HF (0.25 mL)/1 NH_4F (0.257 g)/H_2O (4.25 mL).

$(NH_4)GaPO_4F$ (KTP) was prepared in the same hydrothermal conditions, from the molar ratio 1 GaO(OH)/1 H_3PO_4/1 HF/0.5 GUA/40 H_2O. The mixture was heated at 180 °C for 24 h; the p-KTP phase was obtained for a longer reaction time (4 days). In these synthesis conditions, only a small amount of $(NH_4)GaPO_4F$ is formed in the presence of a powdered unknown phase. The $(NH_4)GaPO_4F$ phase appears as small rhombohedral crystallites and single crystals can be easily isolated for X-ray diffraction analysis. Attempts for producing KTP starting with NH_4F instead of guanidine give a mixture of quartz-type $GaPO_4$ and $NH_4[Ga_2(PO_4)_2(OH)(H_2O)] \cdot H_2O$[18] (leucophosphite structural type).

Characterization. The scanning electron micrographs were taken on a JEOL JSM-5800LV electron microscope using accelerating voltages in the range 15−20 kV coupled with energy-dispersive X-ray emission analysis (Oxford Instrument). The sample $(NH_4)_2Ga_2(PO_4)(HPO_4)F_3$ consists of needle-like crystals stacked in aggregates of about 600 μm (Figure 1a). The SEM micrograph of the KTP sample shows isolated rhombohedral-shaped crystals of about 150 μm in length (Figure 1b).

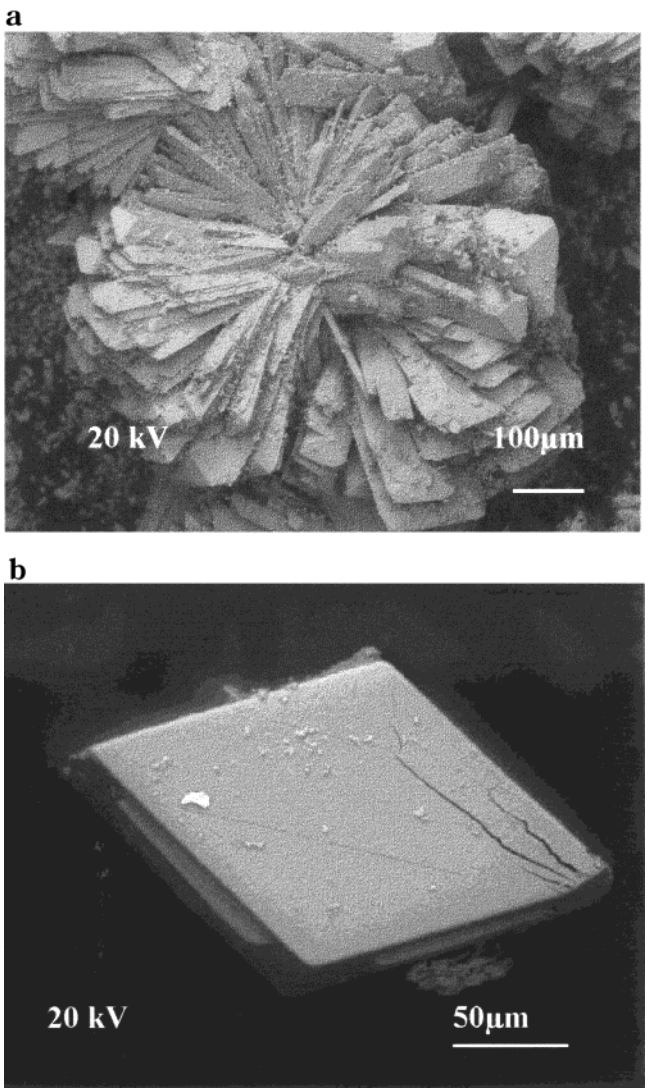

Figure 1. (a) SEM micrograph of a sample of $(NH_4)_2Ga_2(PO_4)(HPO_4)F_3$ (p-KTP) and (b) SEM micrograph of a sample of $(NH_4)GaPO_4F$ (KTP).

The fluorine content of the $(NH_4)_2Ga_2(PO_4)(HPO_4)F_3$ sample was obtained by a potentiometric method with a fluoride ion selective electrode. The chemical analysis gives 13.29% (expected 13.5%) and corresponds to 3 F for 2 $GaPO_4$ units.

Crystal Structure Determinations. A transparent needle-shaped, single crystal of $(NH_4)_2Ga_2(PO_4)(HPO_4)F_3$ was mounted with Araldite on a glass fiber. Room-temperature intensity data collection were performed on a Siemens SMART three-circle diffractometer equipped with a CCD bidimensional detector. The crystal-to-detector distance was 45 mm, allowing for the data collection up to 65° (2θ). Slightly more than one hemisphere of data was recorded. The frames were collected with a scan width of 0.3° in ω and an exposure time of 30 s per frame. Crystal data and details of the data collection are given in Table 1. An empirical absorption correction was applied using the SADABS program[19] based on the method of Blessing.[20] Systematic absences in the reduced data ($00l$, $l \neq 2n$; $h0l$, $h \neq 2n$; $0kl$, $k + l \neq 2n$) were consistent with space groups $Pna2_1$ (no. 33) or $Pnam$ (no. 62). The SHG measurement test was negative and both space groups can be considered. The structure was first solved in the centric space group $Pnam$ by direct methods using the SHELXTL[21] package but

(17) Tordjman, I.; Masse, R.; Guitel, J. C. *Z. Kristallogr.* **1974**, *139*, 103.
(18) Loiseau, T.; Férey, G. *Eur. J. Solid State Inorg. Chem.* **1994**, *31*, 571
(19) Sheldrick, G. M. SADABS, a program for the Siemens Area Detector ABSsorption correction.
(20) Blessing, R. *Acta Crystallogr.* **1995**, *A51*, 33
(21) Sheldrick, G. M. SHELXTL version 5.03, sofware package for the Crystal Structure Determination, 1994.

Table 1. Crystal Data and Structure Refinement for $(NH_4)_2Ga_2(PO_4)(HPO_4)F_3$ (p-KTP) and $(NH_4)GaPO_4F$ (KTP)

identification code	pseudo-KTP	KTP
empirical formula	$F_3Ga_2N_2O_8P_2H_4$	$F_2Ga_2N_2O_8P_2H_4$
formula weight	418.40	399.40
temperature	303(2) K	303(2) K
wavelength	0.71073 Å	0.71073 Å
crystal system	orthorhombic	orthorhombic
space group	$Pna2_1$ (no. 33)	$Pna2_1$ (no. 33)
unit cell dimensions	a = 12.4967(2) Å b = 7.70150(10) Å c = 9.84630(10) Å	a = 12.9207(2) Å b = 6.44000(10) Å c = 10.4147(2) Å
volume, Z	947.64(2) Å^3, 4	866.60(3) Å^3, 4
density (calculated)	2.929 Mg/m^3	3.057 Mg/m^3
absorption coefficient	6.109 mm^{-1}	6.657 mm^{-1}
F(000)	788	752
crystal size	0.46 × 0.05 × 0.05 mm	0.18 × 0.14 × 0.14 mm
θ range for data collection	3.73−32.44°	3.53−32.43°
limiting indices	$-18 \le h \le 17$ $-11 \le k \le 4$ $14 \le l \le 13$	$-18 \le h \le 19$ $-9 \le k \le 6$ $-15 \le l \le 13$
reflections collected	7109	6732
independent reflections	3009 [R(int) = 0.0635]	2788 [R(int) = 0.0278]
refinement method	full-matrix least-squares on F^2	full-matrix least-squares on F^2
data [$I > 2\sigma(I)$][a]/ parameters	2820/155	2216/146
goodness-of-fit on F^2	0.671	0.913
final R indices [$I > 2\sigma(I)$][a]	R1 = 0.0406, wR2 = 0.0985	R1 = 0.0279, wR2 = 0.0785
R indices (all data)	R1 = 0.0422, wR2 = 0.0998	R1 = 0.0297, wR2 = 0.0798
absolute structure parameter	0.004(14)	0.47(2)
extinction coefficient	0.0033(7)	0.0077(5)
largest diff. peak and hole	1.562 and −1.277 e Å^{-3}	0.741 and −0.713 e Å^{-3}

[a] Where wR2 = $[\sum[w(|F_o|^2 - |F_c|^2)^2]/\sum[w(|F_o|^2)^2]]^{1/2}$ and R1 = $\sum||F_o| - |F_c||/\sum|F_o|$.

Table 2. Atomic Coordinates (× 10^4) and Equivalent Isotropic Displacement Parameters (Å^2 × 10^3) for (A) Pseudo-KTP and (B) KTP[a]

	x	y	z	U(eq)
		A. Pseudo-KTP		
Ga(1)	8849(1)	9792(1)	1683(1)	7(1)
Ga(2)	7425(1)	12790(1)	3853(1)	6(1)
P(1)	6898(1)	10849(1)	6654(1)	9(1)
P(2)	9884(1)	11750(2)	4148(1)	6(1)
F(1)	7611(2)	10975(4)	2499(3)	11(1)
F(2)	7180(3)	14600(4)	5168(3)	13(1)
F(3)	9206(3)	11970(4)	897(3)	17(1)
O(1)	7400(3)	11001(5)	5245(4)	13(1)
O(2)	7590(3)	9607(5)	7477(4)	12(1)
O(3)	9624(3)	10075(5)	3347(4)	12(1)
O(4)	5726(3)	10111(4)	6528(5)	18(1)
O(5)	10042(3)	11279(5)	5666(4)	11(1)
O(6)	6767(3)	12616(5)	7371(4)	11(1)
O(7)	8954(3)	13058(5)	4034(4)	10(1)
O(8)	5897(3)	12400(5)	3551(4)	11(1)
N(1)	8623(4)	17585(7)	5313(5)	22(1)
N(2)	4024(4)	11681(8)	8052(7)	30(1)
		B. KTP		
Ga(1)	3852(1)	4971(1)	10015(1)	8(1)
Ga(2)	2475(1)	2526(1)	2499(1)	8(1)
P(1)	5003(1)	3278(1)	2508(2)	7(1)
P(2)	1844(1)	5015(1)	5021(2)	8(1)
F(1)	2747(3)	4702(6)	11271(3)	13(1)
F(2)	2747(3)	5324(6)	8763(3)	13(1)
O(1)	4856(3)	4740(7)	1341(3)	12(1)
O(2)	5162(3)	4661(8)	3697(4)	14(1)
O(3)	4017(2)	1966(4)	2686(4)	12(1)
O(4)	5963(2)	1890(4)	2285(3)	9(1)
O(5)	1167(2)	3108(4)	5344(3)	13(1)
O(6)	1166(2)	6923(5)	4718(3)	12(1)
O(7)	2573(3)	5509(7)	6143(4)	11(1)
O(8)	2557(3)	4528(8)	3852(4)	14(1)
N(1)	3936(4)	7867(7)	3302(7)	49(2)
N(2)	5988(3)	8166(7)	730(4)	27(1)

[a] U(eq) is defined as one-third of the trace of the orthogonalized U_{ij} tensor.

no correct model was found. With the noncentric space group $Pna2_1$, the direct methods gave the location of the gallium and phosphorus atoms. The remaining atoms (F, O, N) were placed from successive Fourier map analyses. The fluorine atoms were located from considerations of the temperature factors of the anions and bond valence calculations. The chemical analysis gives three fluorine atoms for the three crystallographic sites. The hydrogen atoms were not included in the refinements. The final reliability factors, with anisotropic temperature parameters, converge to R1 = 0.0406 and wR2 = 0.0985 (for 2820 reflections $I > 2\sigma(I)$) with 155 parameters for the good enantiomer.

The data collection of NH_4GaPO_4F was performed in a similar way, as summarized in Table 1. The crystallographic system was orthorhombic with the unit cell parameters a = 12.9207(2) Å, b = 6.440(1) Å, c = 10.4147(2) Å, V = 866.60(3) Å^3, which are close to those found for the $KTiOPO_4$ material.[17] Systematic absences indicated space group $Pna2_1$ and $Pnam$ as expected for the KTP type. The structure was refined in the noncentric space group $Pna2_1$ by using the atomic positions of the KTP-isotype NH_4FePO_4F[22] compound with gallium atoms replacing the iron atoms. A refinement with oxygen atoms replacing the fluorine atoms has been tested, and it led to reliability factor R1 = 0.0323. An oxyfluorinated gallophosphate with KTP structure type, $KGaPO_4F_{1-\delta}(OH)_\delta$,[23] has already been isolated and a statistical OH/F occupancy have been suggested for the fluorine sites. We attempted refinements with constraints occ(O) + occ(F) = 1.0 for both fluorine sites, independently, and it converges to an occupancy close to 1.0 for fluorine. Because of the lack of the amount of product obtained during the synthesis, no chemical analysis has been carried out, and the final refinement was performed assuming the fluorine atoms fully occupy the corresponding sites although this phase may exhibit partial occupancy of the fluorine sites by hydroxyl group as in $KGaPO_4F_{1-\delta}(OH)_\delta$.[23] The reliability factors converge to R1 = 0.0279 and wR2 = 0.0785 (for 2216 reflections $I > 2\sigma(I)$) with 146 parameters for the good enantiomer.

The resulting atomic coordinates including isotropic temperature parameters, a selection of bond distances and angles are shown in Tables 2a,b and 3a,b, respectively.

^{31}P and ^{19}F Solid-State NMR Spectroscopies. The nuclear magnetic resonance experiments were performed for the p-KTP material and were recorded with a Bruker DSX500 spectrometer. The ^{31}P spectrum was taken at a spinning rate of 30 kHz (2.5 mm rotor) under the following conditions: ^{1}H nondecoupling; $\pi/2$ pulse length = 2.5 μs; dead time = 5.86 μs; pulse delay (recycle time) = 5 s; resonance frequency = 202.42 MHz; number of scans = 32; number of digitized points = 8 kwords; referencing 0 ppm: H_3PO_4 (85%). The ^{19}F spectrum was acquired at a spinning rate of 30 kHz (2.5 mm rotor) under the following conditions: ^{1}H nondecoupling; $\pi/2$ pulse length = 4 μs; dead time = 4.5 μs; pulse delay (recycle time) = 2 s; resonance frequency = 470.6 MHz; number of scans = 256; number of digitized points = 16 kwords; referencing 0 ppm: $CFCl_3$; solid test sample = NaF. The spectra are decomposed as a sum of Lorentzian−Gaussian lines using the Winfit program simulation.[24]

(22) Loiseau, T.; Lacorre, P.; Calage, Y.; Férey, G. *J. Solid State Chem.* **1994**, *111*, 390.

(23) Harrison, W. T. A.; Phillips, M. L. F.; Stucky, G. D. *Chem. Mater.* **1995**, *7*, 1849.

Table 3. Bond Lengths [Å] and Angles [deg] for (A) Psudo-KTP and (B) KTP

A. Pseudo-KTP[a]		B. KTP[b]	
Ga(1)−O(5)^{i}	1.898(3)	Ga(1)−O(2)^{i}	1.888(4)
Ga(1)−F(3)	1.900(3)	Ga(1)−O(1)^{ii}	1.900(4)
Ga(1)−O(3)	1.915(3)	Ga(1)−F(1)	1.944(3)
Ga(1)−O(6)^{ii}	1.965(4)	Ga(1)−F(2)	1.947(4)
Ga(1)−F(1)	1.967(3)	Ga(1)−O(6)^{iii}	1.987(3)
Ga(1)−F(2)^{ii}	1.976(3)	Ga(1)−O(5)^{iv}	2.049(3)
Ga(2)−F(2)	1.926(3)	Ga(2)−O(8)	1.913(4)
Ga(2)−O(7)	1.930(3)	Ga(2)−O(7)^{v}	1.920(4)
Ga(2)−O(1)	1.944(4)	Ga(2)−F(1)^{vi}	1.929(3)
Ga(2)−F(1)	1.946(3)	Ga(2)−F(2)^{v}	1.956(3)
Ga(2)−O(2)^{iii}	1.948(4)	Ga(2)−O(4)^{vii}	2.002(3)
Ga(2)−O(8)	1.956(3)	Ga(2)−O(3)	2.035(3)
P(1)−O(2)	1.523(4)	P(1)−O(2)	1.539(4)
P(1)−O(1)	1.527(4)	P(1)−O(3)	1.540(3)
P(1)−O(6)	1.542(4)	P(1)−O(4)	1.546(3)
P(1)−O(4)	1.576(4)	P(1)−O(1)	1.549(4)
P(2)−O(8)^{iv}	1.541(3)	P(2)−O(7)	1.535(4)
P(2)−O(7)	1.542(3)	P(2)−O(6)	1.542(3)
P(2)−O(3)	1.547(4)	P(2)−O(5)	1.545(3)
P(2)−O(5)	1.551(4)	P(2)−O(8)	1.559(4)
O(5)^{i}−Ga(1)−F(3)	89.9(2)	O(2)^{i}−Ga(1)−O(1)^{ii}	94.44(9)
O(5)^{i}−Ga(1)−O(3)	97.6(2)	O(2)^{i}−Ga(1)−F(1)	175.0(2)
F(3)−Ga(1)−O(3)	97.4(2)	O(1)^{ii}−Ga(1)−F(1)	90.3(2)
O(5)^{i}−Ga(1)−O(6)^{ii}	95.6(2)	O(2)^{i}−Ga(1)−F(2)	89.6(2)
F(3)−Ga(1)−O(6)^{ii}	170.1(2)	O(1)^{ii}−Ga(1)−F(2)	175.1(2)
O(3)−Ga(1)−O(6)^{ii}	90.0(2)	F(1)−Ga(1)−F(2)	85.57(7)
O(5)^{i}−Ga(1)−F(1)	172.2(2)	O(2)^{i}−Ga(1)−O(6)^{iii}	91.1(2)
F(3)−Ga(1)−F(1)	86.66(14)	O(1)^{ii}−Ga(1)−O(6)^{iii}	92.5(2)
O(3)−Ga(1)−F(1)	89.8(2)	F(1)−Ga(1)−O(6)^{iii}	90.48(14)
O(6)^{ii}−Ga(1)−F(1)	86.9(2)	F(2)−Ga(1)−O(6)^{iii}	90.16(14)
O(5)^{i}−Ga(1)−F(2)^{ii}	92.52(14)	O(2)^{i}−Ga(1)−O(5)^{iv}	90.3(2)
F(3)−Ga(1)−F(2)^{ii}	84.91(14)	O(1)^{ii}−Ga(1)−O(5)^{iv}	87.9(2)
O(3)−Ga(1)−F(2)^{ii}	169.6(2)	F(1)−Ga(1)−O(5)^{iv}	88.09(14)
O(6)^{ii}−Ga(1)−F(2)^{ii}	86.6(2)	F(2)−Ga(1)−O(5)^{iv}	89.31(14)
F(1)−Ga(1)−F(2)^{ii}	80.26(13)	O(6)^{iii}−Ga(1)−O(5)^{iv}	178.51(11)
F(2)−Ga(2)−O(7)	91.03(14)	O(8)−Ga(2)−O(7)^{v}	178.7(2)
F(2)−Ga(2)−O(1)	92.1(2)	O(8)−Ga(2)−F(1)^{vi}	89.3(2)
O(7)−Ga(2)−O(1)	91.5(2)	O(7)^{v}−Ga(2)−F(1)^{vi}	90.6(2)
F(2)−Ga(2)−F(1)	177.60(14)	O(8)−Ga(2)−F(2)^{v}	90.1(2)
O(7)−Ga(2)−F(1)	91.24(13)	O(7)^{v}−Ga(2)−F(2)^{v}	89.98(14)
O(1)−Ga(2)−F(1)	88.63(13)	F(1)^{vi}−Ga(2)−F(2)^{v}	177.9(2)
F(2)−Ga(2)−O(2)^{iii}	86.9(2)	O(8)−Ga(2)−O(4)^{vii}	90.5(2)
O(7)−Ga(2)−O(2)^{iii}	89.8(2)	O(7)^{v}−Ga(2)−O(4)^{vii}	90.80(14)
O(1)−Ga(2)−O(2)^{iii}	178.3(2)	F(1)^{vi}−Ga(2)−O(4)^{vii}	88.2(2)
F(1)−Ga(2)−O(2)^{iii}	92.3(2)	F(2)^{v}−Ga(2)−O(4)^{vii}	93.9(2)
F(2)−Ga(2)−O(8)	93.32(14)	O(8)−Ga(2)−O(3)	89.7(2)
O(7)−Ga(2)−O(8)	175.6(2)	O(7)^{v}−Ga(2)−O(3)	89.0(2)
O(1)−Ga(2)−O(8)	89.0(2)	F(1)^{vi}−Ga(2)−O(3)	90.8(2)
F(1)−Ga(2)−O(8)	84.40(14)	F(2)^{v}−Ga(2)−O(3)	87.2(2)
O(2)^{iii}−Ga(2)−O(8)	89.7(2)	O(4)^{vii}−Ga(2)−O(3)	178.9(2)
O(2)−P(1)−O(1)	107.3(2)	O(2)−P(1)−O(3)	109.3(3)
O(2)−P(1)−O(6)	111.8(2)	O(2)−P(1)−O(4)	110.4(2)
O(1)−P(1)−O(6)	113.1(2)	O(3)−P(1)−O(4)	111.36(11)
O(2)−P(1)−O(4)	110.1(2)	O(2)−P(1)−O(1)	107.22(12)
O(1)−P(1)−O(4)	109.7(3)	O(3)−P(1)−O(1)	109.0(2)
O(6)−P(1)−O(4)	104.8(2)	O(4)−P(1)−O(1)	109.4(2)
O(8)^{iv}−P(2)−O(7)	108.3(2)	O(7)−P(2)−O(6)	109.8(2)
O(8)^{iv}−P(2)−O(3)	109.4(2)	O(7)−P(2)−O(5)	110.3(2)
O(7)−P(2)−O(3)	110.5(2)	O(6)−P(2)−O(5)	110.86(11)
O(8)^{iv}−P(2)−O(5)	111.2(2)	O(7)−P(2)−O(8)	105.91(11)
O(7)−P(2)−O(5)	108.6(2)	O(6)−P(2)−O(8)	109.7(2)
O(3)−P(2)−O(5)	108.9(2)	O(5)−P(2)−O(8)	110.2(2)

[a] Symmetry transformations used to generate equivalent atoms for pseudo-KTP: *i*, $-x+2, -y+2, z-1/2$; *ii*, $-x+3/2, y-1/2, z-1/2$; *iii*, $-x+3/2, y+1/2, z-1/2$; *iv*, $x+1/2, -y+5/2, z$; *v*, $-x+3/2, y+1/2, z+1/2$; *vi*, $-x+3/2, y-1/2, z+1/2$; *vii*, $-x+2, -y+2, z+1/2$; *viii*, $x-1/2, -y+5/2, z$. [b] Symmetry transformations used to generate equivalent atoms for KTP: *i*, $-x+1, -y+1, z+1/2$; *ii*, $x, y, z+1$; *iii*, $-x+1/2, y-1/2, z+1/2$; *iv*, $-x+1/2, y+1/2, z+1/2$; *v*, $-x+1/2, y-1/2, z-1/2$; *vi*, $x, y, z-1$; *vii*, $x-1/2, -y+1/2, z$; *viii*, $-x+1, -y+1, z-1/2$; *ix*, $x+1/2, -y+1/2, z$; *x*, $-x+1/2, y+1/2, z-1/2$.

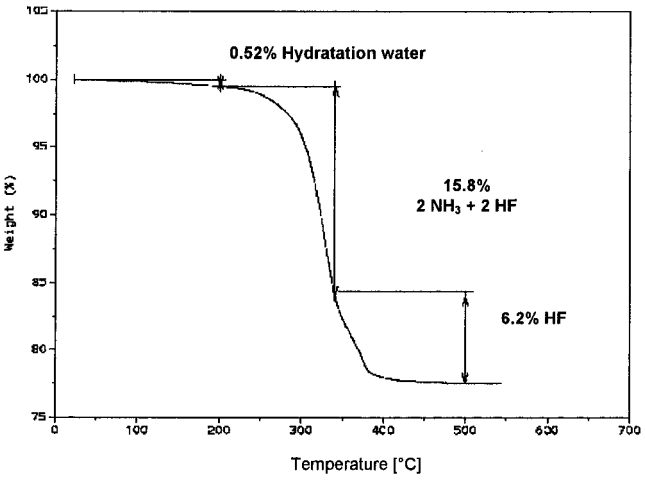

Figure 2. TGA curve of $(NH_4)_2Ga_2(PO_4)(HPO_4)F_3$ (p-KTP) under N_2 (5 °C/min).

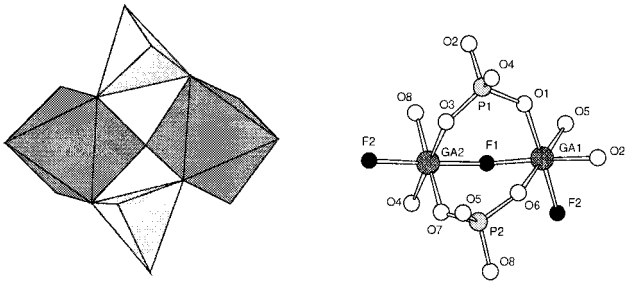

Figure 3. Representation of the asymmetric unit for $(NH_4)GaPO_4F$ (KTP).

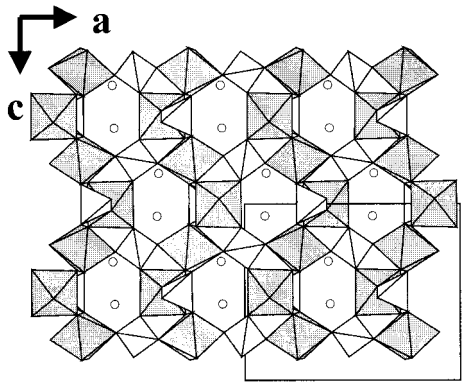

Figure 4. View of the structure of $(NH_4)GaPO_4F$ (KTP) along *b*. Open circles indicate nitrogen atoms of the ammonium groups within the hexagonal 6-ring channels.

TGA Measurement. TGA measurements were carried out on a TA-Instrument type 2050 thermoanalyzer for $(NH_4)_2Ga_2(PO_4)(HPO_4)F_3$. ($N_2$ gas flow; heating rate of 5 °C/min between 30 °C and 600 °C). The TG diagram (Figure 2) shows a single-step weight loss between 250 °C and 375 °C corresponding to 22.0% and can be assigned to the departure of 2 NH_3 and 3 HF (theoretical loss of 22.2%). The XRD pattern of the residue at 600 °C corresponds to the high cristobalite form of $GaPO_4$.

Results

Structure of $(NH_4)GaPO_4F$ (KTP). The structure of $(NH_4)GaPO_4F$ KTP-type is built up from the connection of zigzag chains of GaO_4F_2 octahedra with phosphate groups. The asymmetric unit consists of two PO_4

(24) Winfit/WinNMR suite programs from Bruker-Franzen Co., Bremen, Germany, 1993−1997.

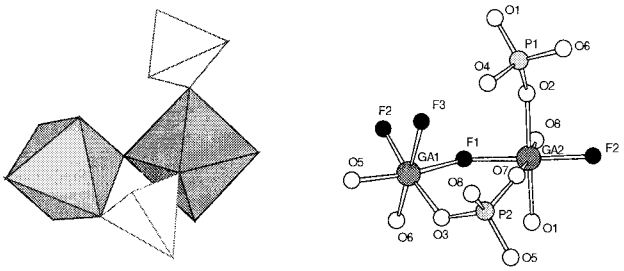

Figure 5. Representation of the asymmetric unit for $(NH_4)_2Ga_2(PO_4)(HPO_4)F_3$ (p-KTP). The atoms O(4) and F(3) are in terminal positions.

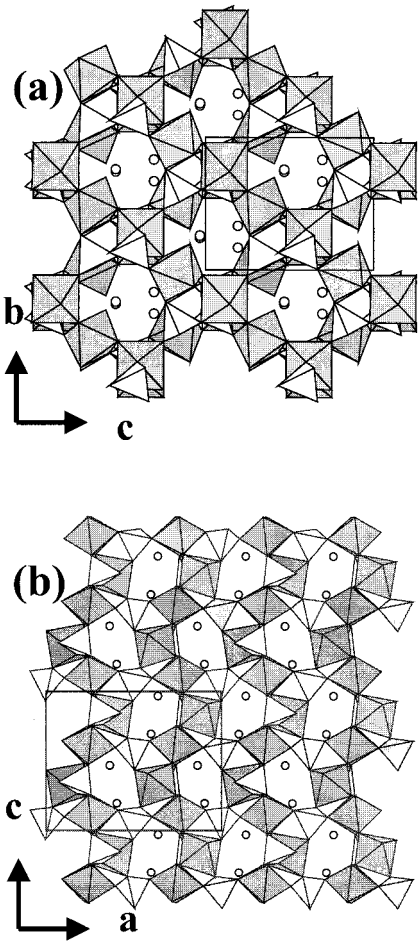

Figure 6. View of the structure of $(NH_4)_2Ga_2(PO_4)(HPO_4)F_3$ (p-KTP): (a) along *a*, showing the 7-ring channels and (b) along *b*, open circles indicate nitrogen atoms of the ammonium groups within the hexagonal 6-ring channels

tetrahedra sharing two of their corners with two GaO_4F_2 octahedra (Figure 3). These two distinct gallium atoms are linked together via a fluorine atom. Within the octahedra, the average Ga−O (≈1.96 Å) distances are close to that of Ga−F (≈1.94 Å) and no short Ga−F linkage is observed as it is the case for the Ti═O titanyl bond in $KTiOPO_4$. The phosphorus atoms are in tetrahedral coordination with average P−O distances of ≈1.54 Å as expected in the phosphate materials. The three-dimensional network is formed by corners sharing of all polyhedra. The Ga−F bonds generate alternating *cis*−*trans* GaO_4F_2 octahedra chains running along [011] and [01$\bar{1}$] connected to PO_4 tetrahedra (Figure 4). The framework delimits 6-ring channels running along [010] and [100] in which the ammonium groups are located.

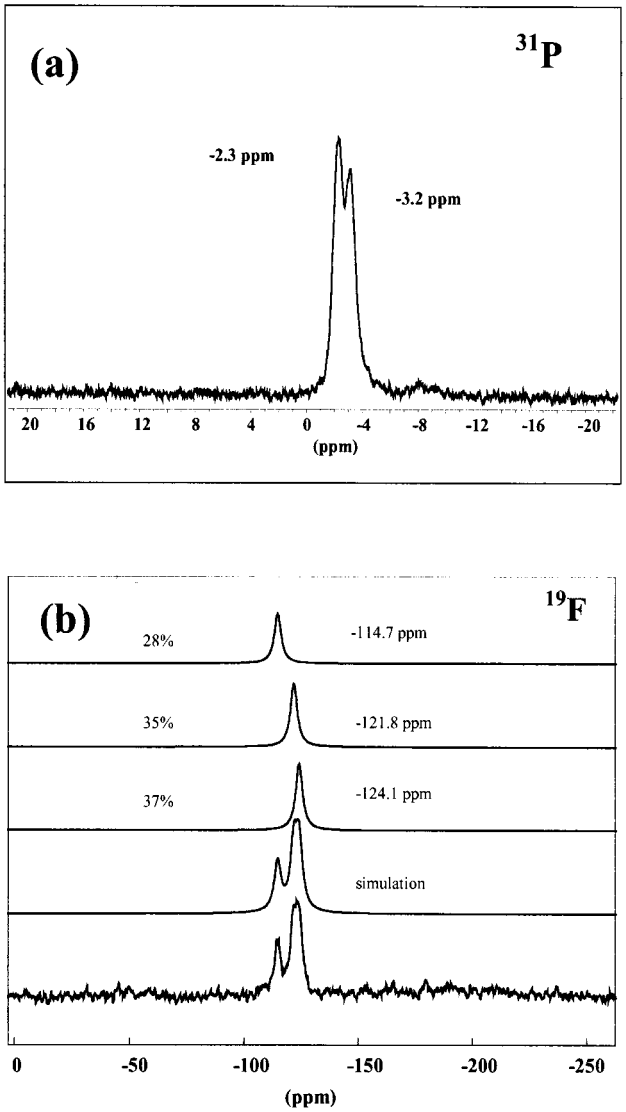

Figure 7. (a) ^{31}P MAS NMR spectrum (470.6 MHz, 14.7 T) and (b) ^{19}F MAS NMR spectrum (202.4 MHz, 14.7 T) of $(NH_4)_2Ga_2(PO_4)(HPO_4)F_3$ (p-KTP).

The examination of the distances between the ammonium groups and the anions shows that N−H···F hydrogen bond interactions are in the same order of magnitude as those of N−H···O.

Structure of $(NH_4)_2Ga_2(PO_4)(HPO_4)F_3$ (Pseudo-KTP). The structure of $(NH_4)_2Ga_2(PO_4)(HPO_4)F_3$ or p-KTP, consists of a three-dimensional connection of PO_4 tetrahedra with GaO_4F_2 and GaO_3F_3 octahedra. The tetrameric basic unit is close to that found in KTP. It is composed of two phosphate groups and two distinct gallium atoms in 6-fold coordination (Figure 5). The $P(2)O_4$ group shares one corner with each of the two gallium polyhedra, whereas the $P(1)O_4$ unit shares only one corner with the Ga(2) gallium polyhedron. The two gallium atoms are linked via a fluorine atom. Both tetrahedrally coordinated phosphorus atoms exhibit an average P−O distance of ≈1.54 Å. The $P(2)O_4$ group shares all its vertexes, whereas the $P(1)O_4$ group shares only three vertexes with gallium polyhedra. It shows that the P−O distances are ranging from 1.523(4) to 1.576(4) Å. The longest P(1)−O bond corresponds to the O(4) oxygen atom which is terminal. Valence sum

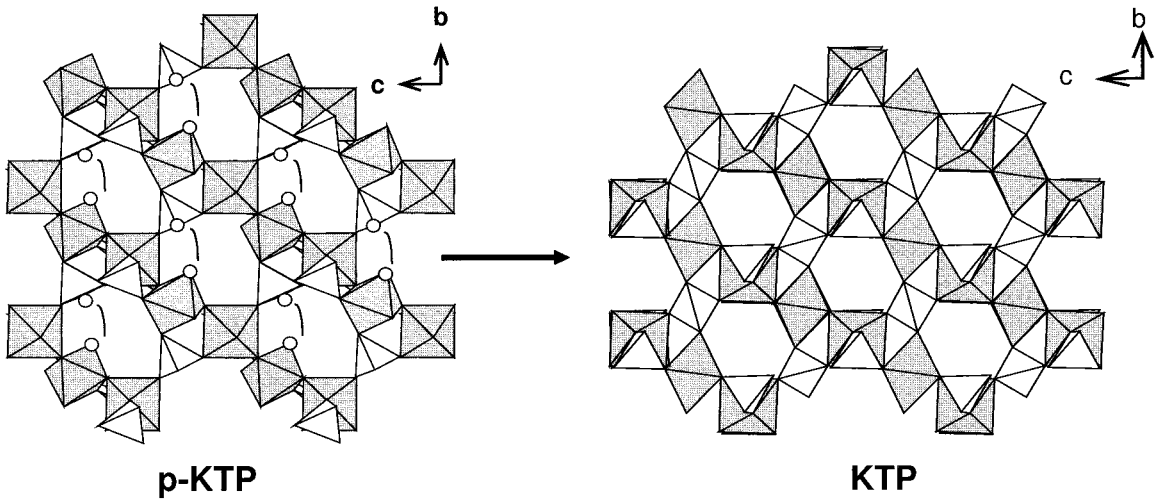

Figure 8. Structural relationships between $(NH_4)_2Ga_2(PO_4)(HPO_4)F_3$ p-KTP type and $(NH_4)GaPO_4F$ KTP type. Open circles indicate the terminal atoms (P−OH and Ga−F) corresponding to the $HP(1)O_4$ and $Ga(1)O_3F_3$ groups. The connection of the terminal atoms P−OH +Ga−F of the p-KTP network leads to the formation of the KTP network.

calculations indicate that this oxygen has an unsatisfied valence due to a hydroxyl group. For the gallium atoms, the situation is similar. The Ga(2) octahedron is almost regular with identical Ga−O and Ga−F distances ($\langle$Ga−O$\rangle$ = 1.94 Å and $\langle$Ga−F$\rangle$ = 1.93 Å). Ga(2) is surrounded by four oxygen and two fluorine atoms. The polyhedron around the Ga(1) is more distorted with a spread of the Ga anions distances: Ga(1) is linked to three oxygen atoms with Ga−O distances ranging from 1.898 to 1.965 Å. Two fluorine atoms bridge the two gallium atoms together; this corresponds to the longer Ga−F distances (Ga−F ≈ 1.97 Å). A third fluorine atom, in terminal position, is characterized by a shorter Ga−F. Such a distance has already been encountered in $GaPO_4$−CJ2[25] in which a terminal Ga−F bond of 1.903 Å occurs. The distances between the two terminal atoms O(4) from $P(1)O_4$ group and F(3) from $Ga(1)O_3F_3$ group is 2.5 Å.

The three-dimensional framework is built up by corner-sharing of the defined tetrameric units, the O(4) and F(3) atoms remaining terminal. The resulting structure is closely related to that of KTP type. One can observe the same *cis*−*trans* $Ga(O,F)_6$ octahedra chains connected to the PO_4 tetrahedra (Figure 6a,b). Along [100] and [001], the PO_4 tetrahedra alternate with the $Ga(O,F)_6$ octahedra, whereas this connection mode does not occur along [010], at variance to the KTP structure. The presence of the terminal atoms as described in the tetrameric unit does not allow for the generation of infinite −P−Ga−P−Ga− etc. chain along this direction. This leads to puckered channels delimited by seven polyhedra along the *a* axis (Figure 6a) and channels delimited by six polyhedra along the *b* axis interconnected with distorted hexagonal channels along the *b* axis (Figure 6b). Ammonium groups are located within these channels. The $N(1)H_4$ group interacts preferentially with the terminal atom F(3) of the gallium octahedron via hydrogen bond ($d_{N(1)\cdots F(3)}$ = 2.74 Å), whereas the $N(2)H_4$ points toward the terminal atom O(4) of the phosphate group ($d_{N(2)\cdots O(4)}$ = 2.87 Å).

NMR Study of the p-KTP. The ^{31}P NMR spectrum (Figure 7a) indicates two resonance peaks at −2.3 and −3.2 ppm. The chemical shift values are related to phosphorus in tetrahedral surrounding in gallium phosphates materials.[25−27] The two peaks, with the expected intensity ratio of 1/1, can be attributed to the two inequivalent crystallographic sites for phosphorus in the structure.

The ^{19}F MAS NMR spectrum of the p-KTP compound (Figure 7b) shows two distincts signals at −114.7 ppm and −123 ppm with the intensity ratio of 1/2, respectively. The observed chemical shift range is in agreement with Ga−F−Ga bridging position as in the fluorinated gallium phosphates of the ULM-n series[26,27] or Ga−F terminal position as in $GaPO_4$-CJ2.[28] The broader signal at −123 ppm can be deconvoluted with two components at −121.8 and −124.1 ppm with intensity ratio close to 1. The resulting ratio for the three lines is therefore 1/1/1. These three resulting components can be attributed to the three inequivalent crystallographic sites for fluorine atoms of the structure of p-KTP. However, the values of the chemical shift does not allow for the full assignment of these peaks to the three crystallographic sites. The chemical shifts are observed in the range from −93.1 to −112.4 ppm in the case of bridging fluorine (in ULM-3 or ULM-4) and −112.9 ppm in the case of terminal position ($GaPO_4$-CJ2). 2D techniques as radio-frequency dipolar recoupling (RFDR) will be necessary to fully elucidate the assignment of the three resonance peaks. The structure shows the fluorine F(3) interacts preferentially via hydrogen bond with the ammonium groups occluded in the tunnels, whereas the two other fluorine F(1) and F(2) are in bridging position. The close structural situation of the two latter and the distribution of chemical shifts suggest that the bridging fluorine atoms correspond to the doublet at δ = −123 ppm and therefore the terminal fluorine F(3) site could be attributed to the single signal at −114.7 ppm.

(25) Férey, G.; Loiseau, T.; Lacorre, P.; Taulelle, F. *J. Solid State Chem.* **1993**, *105*, 179.

(26) Loiseau, T.; Taulelle, F.; Férey, G. *Microporous Mater.* **1997**, *9*, 83.

(27) Loiseau, T.; Taulelle, F.; Férey, G. *Microporous Mater.* **1996**, *5*, 365.

(28) Loiseau, T. Thesis Dissertation, University of Maine, Le Mans, France 1994.

Discussion

The gallium compounds KTP and p-KTP crystallize in the orthorhombic system and are described in the same noncentric space group $Pna2_1$. The cell volumes are quite similar (866.60(3) Å^3 for KTP and 947.67(2) Å^3 for p-KTP) and the volume difference comes from one additional anion in the p-KTP framework. The composition formula are $Ga_2P_2X_{10}$ and $Ga_2P_2X_{11}$ for KTP and p-KTP, respectively (X corresponds to O^{2-}, OH^-, or F^-).

As shown in Figures 4 and 6, the structure of p-KTP exhibits a more distorted three-dimensional network than that of KTP. The channels of the KTP network have regular hexagonal shape along [100] and [010], whereas the hexagonal tunnel along [010] is more distorted.

From these structural considerations, the framework of p-KTP derives from that of KTP. In the structure of p-KTP, the condensation "P−OH + F−Ga" is not complete for one of the phosphorus and gallium atoms, as shown by the occurrence of the Ga−F and P−OH terminal bonds. Figure 8 indicates that the condensation of this type of bond together with slight rotations of the corresponding PO_4 tetrahedra and GaO_3F_3 octahedra would lead to the building of the KTP network. The resulting Ga−O−P bridge could be formed by following this process:

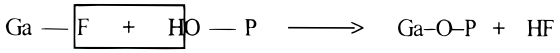

In the p-KTP phase, the existence of the strong terminal fluorine−ammonium interactions seems to be a factor limiting the condcondensation process. In the case of the higher fluorine content (Ga/F < 1), the KTP network cannot be formed due to the NH_4−F pair. In this way, p-KTP may be presented as the fluorolysis product of KTP, which may create the first attack of the Ga−O−P bonds.

Acknowledgment. We thank Dr. Alain Ibanez (Laboratoire de Cristallographie, Grenoble) for the SHG experiments.

Supporting Information Available: Anisotropic displacement parameters and structure factors for p-KTP and KTP. This material is available free of charge via the Internet at http://pubs.acs.org.

CM991177Z